

# From sparse to dense functional time series: phase transitions of detecting structural breaks and beyond

Leheng Cai\* and Qirui Hu\*<sup>†</sup>

**Abstract:** We develop a novel methodology for detecting abrupt break points in mean functions of functional time series, adaptable to arbitrary sampling schemes. By employing B-spline smoothing, we introduce  $\mathcal{L}_\infty$  and  $\mathcal{L}_2$  test statistics based on a smoothed cumulative summation (CUMSUM) process, and derive the corresponding asymptotic distributions under the null and local alternative hypothesis, as well as the phase transition boundary from sparse to dense. We further establish the convergence rate of the proposed break point estimators and conduct statistical inference on the jump magnitude based on the estimated break point, also applicable across sparsely, semi-densely, and densely, observed random functions. Extensive numerical experiments validate the effectiveness of the proposed procedures. To illustrate the practical relevance, we apply the developed methods to analyze electricity price data and temperature data.

**Keywords:** B-spline, Change point, CUMSUM statistics, Functional time series, Phase transition

---

\*Department of Statistics and Data Science, Tsinghua University

<sup>†</sup>Corresponding author: hqr20@mails.tsinghua.edu.cn

# 1 Introduction

Functional time series analysis has emerged as a prominent field in modern statistics, with models and methodologies being applied across various disciplines, such as neuroscience, sociology, economics, and environmental science. Standard references include Bosq (2000) and Horváth and Kokoszka (2012).

Stationarity is a common assumption in the existing literature on functional time series; see Hörmann and Kokoszka (2010), Horváth et al. (2013) and Hu and Li (2024). However, some real-world functional data collected in timely order exhibit structural breaks, leading to a violation of the stationarity assumption. An example of such data is illustrated in Figure 1, which displays the daily electricity price-demand data of German in 2011. Due to the Fukushima nuclear leak in Japan, the German government immediately enacted a new electricity supply policy on March 15, leading to a abrupt shift in the electricity price-demand structure. A detailed analysis of this dataset is referred to section 6.

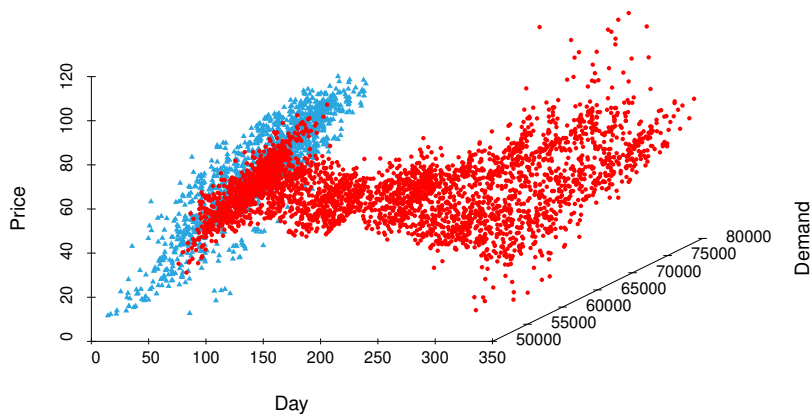


Figure 1: Daily electricity price-demand data of German in 2011. Before March 15, triangle markers; after March 15, circle markers.

The following model summarizes the key features of such observed data  $\{(X_{ij}, Y_{ij})\}_{i,j=1}^{n, N_i}$ ,

$$Y_{ij} = m_i(X_{ij}) + \xi_i(X_{ij}) + \sigma(X_{ij})\varepsilon_{ij}, \quad i = 1, \dots, n, j = 1, \dots, N_i, \quad (1.1)$$

in which the deterministic functions  $\{m_i(\cdot)\}_{i=1}^n$  denotes the mean functions. The functions  $\{\xi_i(\cdot)\}_{i=1}^n$  form a stationary sequence of square-integrable stochastic processes with mean zero over  $[0, 1]$ , which can be viewed as  $\mathcal{L}^2[0, 1]$ -valued random elements. Technically, one has  $\xi_i(x) \in \mathcal{L}^2[0, 1]$  almost surely, satisfying  $\mathbb{E} \int_0^1 \xi_i^2(x) dx < \infty$ . The discrete grids  $\{X_{ij}\}_{i,j=1}^{n, N_i}$  denotes the locations where the random trajectories  $\{\xi_i(\cdot)\}_{i=1}^n$  are recorded, and are i.i.d. copies of  $X$  with density  $f(\cdot)$ . The measurement errors  $\varepsilon_{ij}$ 's are i.i.d. random variables such that  $\mathbb{E}(\varepsilon_{ij}) = 0$  and  $\text{Var}(\varepsilon_{ij}) = 1$ , with variance function  $\sigma^2(\cdot)$ . Besides,  $\{N_i\}_{i=1}^n$  is an array of i.i.d. random variables, taking values in  $\mathbb{Z}_+$ , and  $\mathbb{P}(N_i > 1) > 0$ , and the sets  $\{\xi_i(\cdot)\}_{i=1}^n$ ,  $\{X_{ij}\}_{i=1, j=1}^{n, N_i}$ , and  $\{\varepsilon_{ij}\}_{i=1, j=1}^{n, N_i}$  are mutually independent. While  $\{N_i\}_{i=1}^n$  is assumed to be an i.i.d. array, we do not require  $\mathbb{E}(N_i)$  is bounded, but it can grow to infinity as  $n$  increases.

A fundamental and important task is to test for the presence of structural breaks in mean functions over time, and further estimate the locations of the break if exists. To address this critical issue, we first consider the following break point testing problem in mean functions, where the null and alternative hypotheses are defined as:

$$H_0 : m_1 = \dots = m_n \quad \text{versus} \quad H_1 : m_1 = \dots = m_{k_0} \neq m_{k_0+1} \dots = m_n. \quad (1.2)$$

Here,  $k_0$  is the break point such that  $k_0/n \in (\epsilon, 1 - \epsilon)$  for some fixed  $\epsilon \in (0, 1/2)$ .

The initial approach relies on projection methods to estimate functional principal component (FPC) scores and then transforms the hypothesis in (1.2) into a finite-dimensional testing problem, as discussed in Aue et al. (2009) and Berkes et al. (2009). These methods require consistent estimators for FPC scores and appropriate truncation for the number

of FPCs. Also, the projection approach cannot handle the cases when the jump (defined below) is orthogonal to the FPCs. To proceed, Aue et al. (2018) proposed a CUMSUM test statistic based on the  $\mathcal{L}_2$ -norm, employing the weak invariance principle in Hilbert space  $\mathcal{L}^2[0, 1]$  to avoid dimension reduction. This pioneering research has been widely applied to detect structural breaks in other complex types of functional data, including high-dimensional, spatially correlated, and long-range dependent cases, as illustrated in Li et al. (2023), Wang et al. (2023), and Baek et al. (2024) respectively. Power enhanced methods have also been considered, see Jiao et al. (2023). Additionally, generalized CUMSUM processes have been adapted for estimating multiple break points, as discussed in Rice and Zhang (2022), Bastian et al. (2023), and Harris et al. (2022). However, the aforementioned literature on testing break points focuses on ideal scenarios where trajectories can be fully collected, whereas in practice, recordings are always occur only at regular or random locations. Recently, Hu (2024) addressed the break point analysis of functional variance functions based on data contaminated by measurement errors, by applying B-spline pre-smoothing and kernel methods to asymptotically ignore the noise effect in a dense setting. Moreover, Bai et al. (2024) developed testing procedures for locally stationary functional time series without a pre-smoothing step, accommodating both dense and semi-dense scenarios. These studies, however, only consider regularly recorded data and assume that the sampling frequency be of a comparable order to the sample size  $n$ .

On the other hand, functional data analysis from sparse to dense and related phase transitions are attracting increasing attention. Zhang and Wang (2016) conducted an in-depth analysis of mean and covariance functions, meticulously investigating the convergence rates and point-wise asymptotic normality transitioning from sparse to dense functional data. They introduced subcategories such as sparse, semi-dense and dense, based on the

achievement of the  $n^{-1/2}$  rate and the neglect of asymptotic bias. Sharghi Ghale-Joogh and Hosseini-Nasab (2021) explored the estimation of mean derivatives in longitudinal and functional data across different sampling schemes. Besides, Cai and Yuan (2011) and Berger et al. (2023) investigated the optimal rates for estimating the mean function in the  $\mathcal{L}_2$  and  $\mathcal{L}_\infty$  norms, respectively. More recently, Zhang and Li (2022) delved into a unified principal component analysis for sparse and dense functional data, especially under conditions of spatial dependency. Guo et al. (2023) achieved significant breakthroughs in non-asymptotic mean and covariance estimation within high-dimensional functional time series. From the statistics inference perspective, Cai and Hu (2024a) constructed simultaneous confidence bands for the mean function transitioning from sparse to dense, utilizing B-spline and other orthogonal series estimator. In the realm of break points analysis in functional data, to the best of our knowledge, only Madrid Padilla et al. (2022) and Xue et al. (2024) have considered the estimation of break points in mean function and covariance structures, respectively, under the assumption of existing breaks. However, for testing whether there is a structural break in the mean function, existing work typically assume specific sampling schemes and develop corresponding procedures based on their restrictive assumptions, thus no general approaches without sampling restrictions have been studied yet.

In this paper, one innovation that should be emphasized is that our developed approach provides a unified framework for testing the break point in functional time series, valid under a general dependence structure and allowing for arbitrary sampling designs. By employing B-spline estimators for the partial and global mean functions, we construct a smoothed CUMSUM process. Beyond the conventional  $\mathcal{L}_2$ -norm based test statistic, we also introduce an  $\mathcal{L}_\infty$ -norm based test statistic. Although the theoretical properties of  $\mathcal{L}_2$  statistics have been widely studied, analyzing  $\mathcal{L}_\infty$  statistics is more challenging due to the

absence of an inner product in the space  $\mathcal{C}[0, 1]$ . Each of these two statistics has its own advantages depending on the features of the jump. Our work rigorously derives the general asymptotic distributions of the proposed test statistics under the null and local alternatives, and further establishes the phase transition boundaries for sparsely, semi-densely, and densely observed data. Since the smoothed CUMSUM process we constructed might not be tight, leading to an additional gap to weak convergence results, we alternatively provide Gaussian approximation varying with time  $n$ . The derived theory is consistent with the specific cases, such as those discussed in dense or semi-dense scenarios of Bai et al. (2024) and fully observed scenarios of Aue et al. (2018). Under certain conditions, the approximating Gaussian fields will reduce to the ones in both papers. Recent results on sequential Gaussian approximation under physical dependence from Mies and Steland (2023), the Lévy concentration inequality in Chernozhukov et al. (2015), and properties of splines from De Boor (1978) and Schumaker (2007) are interwoven seamlessly to achieve satisfactory theoretical results.

Additionally, we develop two estimators for break points based on the aforementioned  $\mathcal{L}_\infty$  and  $\mathcal{L}_2$  statistics, and investigate the corresponding convergence rates. Moreover, we are interested in the simultaneous inference of the jump magnitude, defined by  $\Delta(\cdot) = m_{k_0+1}(\cdot) - m_{k_0}(\cdot)$ . A two-step unified simultaneous confidence band (SCB) for the jump magnitude is constructed. SCBs are powerful tools for quantifying the variability of complex functions and making statistical inference, thus it is highly desirable to construct SCBs for the jump magnitude backed by rigorous theory. So far, we have provided a comprehensive methodology for the hypothesis testing problem (1.2), along with subsequent break point location and jump inference, from sparse to dense functional time series.

This paper is organized as follows: Section 2 introduces the construction of the smoothed

CUMSUM process, along with the proposed test statistics, break point estimators, and jump magnitude estimators. Section 3 establishes corresponding asymptotic properties. Section 4 provides detailed descriptions of the implementation. Simulation results and data applications are presented in Sections 5 and 6, respectively. Technical proofs of theoretical results are included in the supplemental materials.

## 2 Methodology

To describe the temporal dependence, following Zhou and Dette (2023) we specify  $\xi_i(\cdot) = H(\cdot, \mathcal{F}_i)$ , where  $H : [0, 1] \times \mathcal{S}^{\mathbb{N}} \rightarrow \mathbb{R}$  is a filter,  $\mathcal{F} = (\dots, e_{i-1}, e_i)$ , and  $\{e_i\}_{i \in \mathbb{Z}}$  is a sequence of i.i.d. random elements within some measurable space  $\mathcal{S}$ . Then, the physical dependence measure of  $\{\xi_i(\cdot)\}_{i \in \mathbb{Z}}$  is defined by:  $\delta_H(i, r) = \sup_{x \in [0, 1]} \|H(x, \mathcal{F}_i) - H(x, \mathcal{F}_i^*)\|_r$ , where  $\mathcal{F}_i^* = (\dots, e_{-1}, e_0^*, e_1, \dots, e_i)$ , and  $e_0^*$  is a copy of  $e_0$  and independent of  $\{e_i\}_{i \in \mathbb{Z}}$ . The long-run covariance function of  $\{\xi_i(\cdot)\}_{i=1}^n$  is expressed as:

$$G(x, x') = \sum_{h=-\infty}^{\infty} \text{Cov}(H(x, \mathcal{F}_h), H(x', \mathcal{F}_0)).$$

Common stationary functional time series models include Functional AR and Functional MA models. The details of their physical dependence measures, as well as examples of other nonlinear functional time series models, are referred to Zhou and Dette (2023) and Dette and Wu (2024).

In the following, denote  $\eta_i(\cdot) = m(\cdot) + \xi_i(\cdot)$  for  $i = 1, \dots, n$ . As pointed in Aue et al. (2018), if one fully observes the random functions  $\{\eta_i(\cdot)\}_{i=1}^n$ , the test statistic could be the squared  $\mathcal{L}_2$ -norm of a CUMSUM process, i.e.,

$$\tilde{S}_n = \max_{1 \leq k \leq n} \left\| \frac{1}{\sqrt{n}} \left( \sum_{i=1}^k \eta_i(x) - \frac{k}{n} \sum_{i=1}^n \eta_i(x) \right) \right\|_{\mathcal{L}_2}^2. \quad (2.1)$$

Under some regular conditions,  $\tilde{S}_n$  weakly converges to some functional of a Gaussian field with covariance function  $(\min\{t, t'\} - tt')G(x, x')$ . For sufficient dense collected data, one may recover the trajectories  $\{\eta_i(\cdot)\}$  by some non-parametric smoothers, denoted by  $\{\hat{\eta}_i(\cdot)\}_{i=1}^n$ , and then considers the squared  $\mathcal{L}_2$ -norm of a plug-in CUMSUM process,

$$\hat{S}_n = \max_{1 \leq k \leq n} \left\| \frac{1}{\sqrt{n}} \left( \sum_{i=1}^k \hat{\eta}_i(x) - \frac{k}{n} \sum_{i=1}^n \hat{\eta}_i(x) \right) \right\|_{\mathcal{L}_2}^2. \quad (2.2)$$

By proving the oracle efficiency property as described in Cao et al. (2012) or Cai and Hu (2024b),  $\hat{S}_n$  is asymptotically equivalent to  $\tilde{S}_n$ . When the recorded location  $X_{ij}$  are fixed and regular, i.e.,  $X_{ij} = j/N$  for all  $i = 1, \dots, n$ , Bai et al. (2024) proposed the following statistics without pre-smoothing and allows the data observed semi-densely,

$$\check{S}_n = \max_{1 \leq k \leq n} \frac{1}{\sqrt{n}N} \sum_{j=1}^N \left( \sum_{i=1}^k Y_{ij} - \frac{k}{n} \sum_{i=1}^n Y_{ij} \right)^2. \quad (2.3)$$

As  $n, N \rightarrow \infty$ , the asymptotically distribution of  $\check{S}_n$  is related to the long-run covariance function  $G(x, x')$  of the processes  $\{\xi_i(\cdot)\}_{i=1}^n$  and the variance function  $\sigma^2(x)$  of the errors  $\varepsilon_{ij}$ 's.

For practically collected data in (1.1), it is hard to approach the conditions of oracle efficiency for  $\hat{S}_n$  in (2.2) when the sampling scheme is not dense enough. Beside, the test statistic  $\check{S}_n$  in (2.3) can not accommodate the settings of irregular design, also their proposed bootstrap method would fail. Therefore, it is strongly motivated to develop a unified theory for the break point testing problem in (1.2), especially for sparse functional times series.

Before introducing our newly proposed statistics, B-spline functions are described below. Let  $\{t_l\}_{l=0}^{J_n+1}$  be a sequence of equally-spaced points, where  $t_l = l/(J_n + 1)$  for  $0 \leq l \leq J_n + 1$ , which divide  $[0, 1]$  into  $J_n + 1$  equal sub-intervals, denoted as  $I_l = [t_l, t_{l+1})$  for  $l = 0, \dots, J_n - 1$ , and  $I_{J_n} = [t_{J_n}, 1]$ . Let  $\mathcal{S}_{J_n}^p = \mathcal{S}_{J_n}^p[0, 1]$  be the polynomial spline space



of order  $p$  over  $\{I_l\}_{l=0}^{J_n}$ , consisting of all functions that are  $(p - 2)$  times continuously differentiable on  $[0, 1]$  and are polynomials of degree  $(p - 1)$  within the sub-intervals  $I_l$ ,  $l = 0, \dots, J_n$ . Let  $\mathbf{B}(x) = \{B_{l,p}(x), \dots, B_{J_n+p,p}(x)\}^\top$  be the  $p$ -th order B-spline basis functions of  $\mathcal{S}_{J_n}^p$ , then  $\mathcal{S}_{J_n}^p = \left\{ \sum_{l=1}^{J_n+p} \lambda_l B_{l,p}(x) : \lambda_l \in \mathbb{R} \right\}$ .

We construct a smoothed CUMSUM process that can adapt to functional time series from sparse to dense by pooling the data points to estimate the partial mean and global mean function separately. For some fixed  $\epsilon \in (0, 1/2)$  and any  $t \in (\epsilon, 1 - \epsilon)$ , the estimation of partial mean function and the global mean function is given by

$$\widehat{m}(t, x) = \arg \min_{g(\cdot) \in \mathcal{S}_{J_n}^p} \frac{1}{[nt]} \sum_{i=1}^{[nt]} \frac{1}{N_i} \sum_{j=1}^{N_i} \{Y_{ij} - g(X_{ij})\}^2, \quad (2.4)$$

$$\widehat{m}(x) = \arg \min_{g(\cdot) \in \mathcal{S}_{J_n}^p} \frac{1}{n} \sum_{i=1}^n \frac{1}{N_i} \sum_{j=1}^{N_i} \{Y_{ij} - g(X_{ij})\}^2. \quad (2.5)$$

The solution to (2.4) and (2.5) are  $\widehat{m}(t, x) = \mathbf{B}^\top(x) \widehat{\boldsymbol{\theta}}_t$  and  $\widehat{m}(x) = \mathbf{B}^\top(x) \widehat{\boldsymbol{\theta}}$  respectively, where

$$\widehat{\boldsymbol{\theta}}_t = \widehat{\mathbf{V}}_t^{-1} \left\{ \frac{1}{[nt]} \sum_{i=1}^{[nt]} \frac{1}{N_i} \sum_{j=1}^{N_i} \mathbf{B}(X_{ij}) Y_{ij} \right\}, \quad \widehat{\mathbf{V}}_t = \frac{1}{[nt]} \sum_{i=1}^{[nt]} \frac{1}{N_i} \sum_{j=1}^{N_i} \mathbf{B}(X_{ij}) \mathbf{B}^\top(X_{ij}).$$

$$\widehat{\boldsymbol{\theta}} = \widehat{\mathbf{V}}^{-1} \left\{ \frac{1}{n} \sum_{i=1}^n \frac{1}{N_i} \sum_{j=1}^{N_i} \mathbf{B}(X_{ij}) Y_{ij} \right\}, \quad \widehat{\mathbf{V}} = \frac{1}{n} \sum_{i=1}^n \frac{1}{N_i} \sum_{j=1}^{N_i} \mathbf{B}(X_{ij}) \mathbf{B}^\top(X_{ij}).$$

Methodologically, different from Madrid Padilla et al. (2022) that assumes that the number of observations is the same across curves and adopts Nadaraya-Watson estimators, we consider more computationally efficient B-spline estimators, which assign different weights  $N_i^{-1}$  to the data points on  $i$ -th trajectory to accommodate different sampling frequency across different trajectories. Similar weighted smoothing estimators can be found in Li and Hsing (2010) and Cai and Yuan (2011). Theoretically, inspired by recent results of sequential Gaussian approximation in high dimensions in Mies and Steland (2023), the definition in (2.4) allows  $\widehat{\boldsymbol{\theta}}_t$  to be expressed as the partial mean of a vector-valued stationary

time series, multiplied on the left by the inverse of an inner product matrix under the null in (1.2). This fact is crucial for constructing Gaussian approximation of the partial mean and global mean estimators.

Then, we adopt the partial mean and global mean to form a smoothed CUMSUM process, and further develop the  $\mathcal{L}_\infty$  and  $\mathcal{L}_2$  statistics,  $T_n$  and  $S_n$ , respectively, to address different types of jump functions.

$$T_n = \sup_{\epsilon \leq t \leq 1-\epsilon} \left\| \frac{[nt]\widehat{m}(t, \cdot)/\sqrt{n} - \sqrt{nt}\widehat{m}(\cdot)}{\sqrt{\mathbf{B}^\top(\cdot)\boldsymbol{\Sigma}\mathbf{B}(\cdot)}} \right\|_\infty, \quad (2.6)$$

$$S_n = \sup_{\epsilon \leq t \leq 1-\epsilon} \left\| \frac{[nt]\widehat{m}(t, \cdot)/\sqrt{n} - \sqrt{nt}\widehat{m}(\cdot)}{\sqrt{\mathbf{B}^\top(\cdot)\boldsymbol{\Sigma}\mathbf{B}(\cdot)}} \right\|_{\mathcal{L}_2}^2, \quad (2.7)$$

where  $\boldsymbol{\Sigma} = \boldsymbol{\Sigma}_1 + \boldsymbol{\Sigma}_2$ ,  $\mathbf{V} = \mathbb{E}\mathbf{B}(X)\mathbf{B}^\top(X)$ , and

$$\boldsymbol{\Sigma}_1 = \mathbf{V}^{-1}\mathbb{E}\{(N-1)/N\}\mathbb{E}\mathbf{B}(X)\mathbf{B}^\top(X')G(X, X')\mathbf{V}^{-1}, \quad (2.8)$$

$$\boldsymbol{\Sigma}_2 = \mathbf{V}^{-1}\mathbb{E}(N^{-1})\mathbb{E}\mathbf{B}(X)\mathbf{B}^\top(X)\{G(X, X) + \sigma^2(X)\}\mathbf{V}^{-1}.$$

Here,  $X'$  is an i.i.d. copy of  $X$ . It is worth noticing that the range of supreme with respect to  $t$  can be relaxed to  $[\epsilon, 1]$ , while the lower bound needs to be strictly positive, since one needs the inverse of  $\widehat{\mathbf{V}}_t$  to be well defined. Observe that the smoothed CUMSUM process, as a function of  $t$ , tends to grow large in terms of either  $\mathcal{L}_\infty$  or  $\mathcal{L}_2$  norm at the rescaled break point  $\tau_0 = \lim_{n \rightarrow \infty} k_0/n$ . Hence, one rejects the null when the value of  $T_n$  or  $S_n$  is large. Notice that the numerators in  $T_n$  and  $S_n$  form a CUMSUM process, which can be approximated by (2.1) and (2.2) in the completely and densely observed functional time series setting. However, an additional unknown term appears in the denominators and serves as a normalizer, preventing the statistics from diverging, particularly in sparse data scenarios. A detailed discussion on  $\mathbf{B}^\top(\cdot)\boldsymbol{\Sigma}\mathbf{B}(\cdot)$  is provided in Section 3 and Lemma 2.3 in the supplemental material. For practical implementation, we estimate  $\boldsymbol{\Sigma}$  and then substitute the estimator back into the expression; details of this procedure are given in Section 4.1.

The previous CUMSUM statistics mainly focus on the  $\mathcal{L}_2$  norm (Aue et al. (2018)), partially because the weak invariance principle is not hard to derive in Hilbert space, while Gaussian approximation in Banach space presents more challenge. For high-dimensional inference as discussed in Li et al. (2024), an  $\ell_2$ -based test statistic is generally more powerful in detecting weak dense signals compared to an  $\ell_\infty$  one, while in the case of sparse signals, an  $\ell_\infty$  type statistic appears better. The same phenomenon also appears in function space.

Once the testing procedure rejects the null hypothesis of no abrupt change in the mean function, it is then of interest to locate the break point. The  $\mathcal{L}_\infty$ -based and  $\mathcal{L}_2$ -based break point estimators are defined accordingly,

$$\widehat{k}_{n,2} = \arg \max_{\epsilon n \leq k \leq (1-\epsilon)n} \left\| \mathbf{B}^\top(\cdot) \widehat{\mathbf{V}}^{-1} \left\{ \sum_{i=1}^k \frac{1}{N_i} \sum_{j=1}^{N_i} \mathbf{B}(X_{ij}) Y_{ij} - \frac{k}{n} \sum_{i=1}^n \frac{1}{N_i} \sum_{j=1}^{N_i} \mathbf{B}(X_{ij}) Y_{ij} \right\} \right\|_{\mathcal{L}_2}^2, \quad (2.9)$$

$$\widehat{k}_{n,\infty} = \arg \max_{\epsilon n \leq k \leq (1-\epsilon)n} \left\| \mathbf{B}^\top(\cdot) \widehat{\mathbf{V}}^{-1} \left\{ \sum_{i=1}^k \frac{1}{N_i} \sum_{j=1}^{N_i} \mathbf{B}(X_{ij}) Y_{ij} - \frac{k}{n} \sum_{i=1}^n \frac{1}{N_i} \sum_{j=1}^{N_i} \mathbf{B}(X_{ij}) Y_{ij} \right\} \right\|_{\mathcal{L}_\infty}.$$

When constructing the break point estimators, we avoid using the partial version of the inner product matrix  $\widehat{\mathbf{V}}_t$ , and instead use the global version of  $\widehat{\mathbf{V}}$ , which technically facilitates proving the convergence rate of the  $\mathcal{L}_2$ -based break point estimator  $\widehat{k}_{n,2}$ .

Although the convergence rate of  $\widehat{k}_{n,\infty}$  is slower than  $\widehat{k}_{n,2}$  asymptotically in Theorem 3.3, it has better empirical performance in special cases, as shown in Figure 2. The jump magnitude are set as  $\Delta(x) = a$  and  $\Delta(x) = a\sqrt{\beta_{10,1000}(x) + \beta_{1000,1000}(x) + \beta_{1000,10}(x)}/\sqrt{3}$ , where  $\beta_{\cdot,\star}(x)$  is the probability density function of  $\beta$ -distribution. Following the empirical results, one can find when  $\|\Delta(x)\|_\infty = \|\Delta(x)\|_{\mathcal{L}_2}$  (constant functions), the performance of  $\widehat{k}_{n,2}$  will be significantly better than  $\widehat{k}_{n,\infty}$  due to the faster convergence rate. On the other hand, when  $\|\Delta(x)\|_\infty$  much greater than  $\|\Delta(x)\|_{\mathcal{L}_2}$  (functions with spark peak), the mean absolute error (MAE) of  $\widehat{k}_{n,\infty}$  is less than  $\widehat{k}_{n,2}$ .

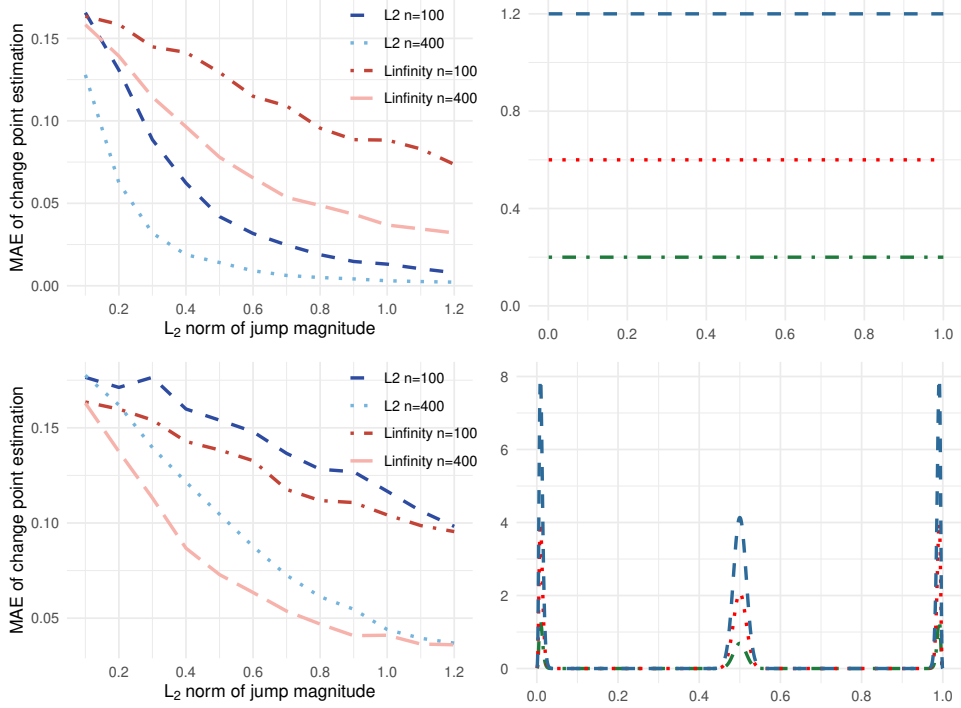


Figure 2: Examples of empirical performance of estimator  $\hat{k}_{n,\infty}$  and  $\hat{k}_{n,2}$  with MAE (left panel) with corresponding jump magnitude (right panel,  $\mathcal{L}_2$  norm of jump magnitude, line for 1.2, dotted for 0.6, dashed for 0.2).

Moreover, given an estimation of the break point, denoted by  $\hat{k}_n$ , we aim to estimate and conduct statistical inference for the jump function  $\Delta(\cdot)$ , as well as the mean functions before and after the break point. For the obtained break point estimation  $\hat{k}_n$ , we estimate  $\Delta(\cdot)$  as

$$\hat{\Delta}_n(\cdot) = \hat{m}_{\hat{k}_n}(\cdot) - \hat{m}_{\hat{k}_n+1}(\cdot), \quad (2.10)$$

where

$$\hat{m}_{\hat{k}_n}(\cdot) = \arg \min_{g(\cdot) \in \mathcal{S}_{J_n}^p} \frac{1}{\hat{k}_n} \sum_{i=1}^{\hat{k}_n} \frac{1}{N_i} \sum_{j=1}^{N_i} \{Y_{ij} - g(X_{ij})\}^2, \quad (2.11)$$

$$\hat{m}_{\hat{k}_n+1}(\cdot) = \arg \min_{g(\cdot) \in \mathcal{S}_{J_n}^p} \frac{1}{n - \hat{k}_n} \sum_{i=\hat{k}_n+1}^n \frac{1}{N_i} \sum_{j=1}^{N_i} \{Y_{ij} - g(X_{ij})\}^2. \quad (2.12)$$

### 3 Main results

#### 3.1 Asymptotic properties of structural break detectors

For a real number  $\nu \in (0, 1]$  and integer  $q \in \mathbb{N}$ ,  $d \in \mathbb{N}_+$ , write  $\mathcal{H}_{q,\nu}([0, 1]^d)$  as the space of  $(q, \nu)$ -Hölder continuous functions on  $[0, 1]^d$ , that is,

$$\mathcal{H}_{q,\nu}([0, 1]^d) = \left\{ h : [0, 1]^d \rightarrow \mathbb{R}, \|h\|_{q,\nu} = \sup_{t \neq s \in [0,1]^d, \alpha \in \mathbb{N}^d, \|\alpha\|_1 = q} \frac{|\partial^\alpha h(t) - \partial^\alpha h(s)|}{\|t - s\|_2^\nu} < \infty \right\}.$$

To derive asymptotic properties, some mild assumptions are introduced first.

(A1) Assume that  $m_i(\cdot) \in \mathcal{H}_{q,\nu}[0, 1]$ ,  $i = k_0, k_0 + 1$ , for some integer  $q > 0$  and some positive real number  $\nu \in (0, 1]$ . In the following, denote  $q^* = q + \nu$ .

(A2) The density function  $f(\cdot)$  of  $X$  is bounded above and away from zero, i.e.,  $c_f \leq \inf_{x \in [0,1]} f(x) \leq \sup_{x \in [0,1]} f(x) \leq C_f$  for some positive constants  $c_f$  and  $C_f$ .

(A3) The variance function  $\sigma^2(\cdot)$  is uniformly bounded, and  $\mathbb{E}|\epsilon_i|^{r_1} < \infty$  for some integer  $r_1 \geq 3$ .

(A4) The long-run covariance function  $G(\cdot, \cdot) \in \mathcal{H}_{0,\mu}[0, 1]^2$  for some  $\mu \in (0, 1]$ ,  $\inf_{x \in [0,1]} G(x, x) \geq c_G$  for some positive constant  $c_G$ , and  $\sup_{x \in [0,1]} \mathbb{E}|\eta(x)|^{r_2} < \infty$  for some integer  $r_2 \geq 3$ .

(A5) For some  $\beta \geq 3$  and  $r_2$  in (A4), the dependence measure  $\delta_H(i, r_2) = \mathcal{O}(i^{-\beta})$ .

(A6) Suppose that the spline order is  $p \geq q^*$ . Let  $r = \min\{r_1, r_2\}$  and  $a_n = \log^{1/2} n$ . When  $\mathbb{E}(N^{-1})J_n \gg 1$ ,  $J_n^{-q^* - 1/2} n^{1/2} \mathbb{E}^{-1/2}(N^{-1})a_n = \mathcal{O}(1)$ , and

$$J_n^{\frac{7r-6}{3r-2}} \left\{ \sum_{s=1}^r \mathbb{E}(N^{s-r}) J_n^{-s} \right\}^{2/r} n^{-\frac{r-2}{3r-2}} \mathbb{E}^{-1}(N^{-1})a_n^2 \rightarrow 0.$$

When  $\mathbb{E}(N^{-1})J_n \lesssim 1$ ,  $J_n^{-q^*} n^{1/2} a_n = \mathcal{O}(1)$ , and

$$J_n^{\frac{10r-8}{3r-2}} \left\{ \sum_{s=1}^r \mathbb{E}(N^{s-r}) J_n^{-s} \right\}^{2/r} n^{-\frac{r-2}{3r-2}} a_n^2 \rightarrow 0.$$

(A6') Let  $a_n = 1$  in (A6).

The smoothness of the mean functions and covariance function in Assumptions (A1) and (A4) are standard conditions in literature; see Cao et al. (2012) and Cai and Hu (2024a) for instance. Assumption (A2) is common for random design, such as in Li and Hsing (2010) and Cai and Yuan (2011). Assumptions (A3) and (A4) impose moment conditions on the stochastic process  $\eta_i(\cdot)$  and the measurement error  $\epsilon_{ij}$ , with similar conditions discussed in Zhang and Wang (2016) and Zhang and Li (2022). Since we do not impose a smoothness condition on  $\sigma(\cdot)$ , the partial measurement error framework in Bai et al. (2024) can also be applied. Assumption (A5) involves a polynomial rate of decay for the physical dependence measure, ensuring the weak dependence of the functional time series. Similar polynomial decaying rates can be also found in Cui and Zhou (2023) and Zhou and Dette (2023). The range of parameters specified in Assumptions (A1), (A3), and (A4) is detailed in Assumption (A6).

Let  $\mathcal{Z}_n(t, x)$  be a sequence of Gaussian random fields with mean zero and covariance function  $\text{Cov}(\mathcal{Z}_n(t, x), \mathcal{Z}_n(t', x')) = (\min\{t, t'\} - tt') \mathbf{B}^\top(x) \boldsymbol{\Sigma} \mathbf{B}(x')$ .

**Theorem 3.1.** *Suppose that the null hypothesis  $H_0$  holds.*

(a) *Under Assumptions (A1)-(A6), as  $n \rightarrow \infty$ ,*

$$\sup_{z \in \mathbb{R}} \left| \mathbb{P}(T_n \leq z) - \mathbb{P} \left( \sup_{\epsilon \leq t \leq 1-\epsilon} \sup_{x \in [0,1]} \frac{|\mathcal{Z}_n(t, x)|}{\sqrt{\mathbf{B}^\top(x) \boldsymbol{\Sigma} \mathbf{B}(x)}} \leq z \right) \right| \rightarrow 0. \quad (3.1)$$

(b) *Under Assumptions (A1)-(A5) and (A6'), as  $n \rightarrow \infty$ ,*

$$\sup_{z \in \mathbb{R}} \left| \mathbb{P}(S_n \leq z) - \mathbb{P} \left( \sup_{\epsilon \leq t \leq 1-\epsilon} \int_0^1 \frac{\mathcal{Z}_n^2(t, x)}{\mathbf{B}^\top(x) \boldsymbol{\Sigma} \mathbf{B}(x)} dx \leq z \right) \right| \rightarrow 0. \quad (3.2)$$

Theorem 3.1 describes null distribution of the test statistics  $T_n$  in (2.6) and  $S_n$  in (2.7), which is uniformly approximated by the distribution of certain functionals of a sequence of

zero-mean Gaussian fields. Since no restrictions are imposed on the relationship between  $n$  and  $N_i$  in Assumptions (A1)-(A6), Theorem 3.1 contains scenarios with arbitrary sampling schemes from sparse to dense. An extreme case is  $m_i(\cdot) \equiv m_i$ . With a slight violation of the range of the number of knots in Assumption (A6), the partial mean (2.4) and global mean (2.5) using the constant spline with  $J_n + p = 1$  will degenerate to  $\widehat{m}(t, \cdot) = [nt]^{-1} \sum_{i=1}^{[nt]} Y_{i1}$ ,  $\widehat{m}(\cdot) = n^{-1} \sum_{i=1}^n Y_{i1}$ , and the term  $\mathbf{B}^\top(x)\boldsymbol{\Sigma}\mathbf{B}(x')$  shrinks to a constant scalar. In this case,  $T_n$  and  $S_n$  weakly converge to the maximum absolute value and the maximum value of the square of Brownian bridges on  $[\epsilon, 1-\epsilon]$  respectively, as in the classical change point theory in time series.

The covariance function of the approximating Gaussian processes can be decomposed into the sum of  $\mathbf{B}^\top(x)\boldsymbol{\Sigma}_1\mathbf{B}(x')$  and  $\mathbf{B}^\top(x)\boldsymbol{\Sigma}_2\mathbf{B}(x')$ , reflecting on the definition of the matrix  $\boldsymbol{\Sigma} = \boldsymbol{\Sigma}_1 + \boldsymbol{\Sigma}_2$ . The former represents the spline approximation of the long-run covariance function  $G(x, x')$ , interpreted as the influence of dependency of  $\{\xi_i(X_{ij})\}_{i,j=1}^{n, N_i}$  both within and between curves  $\{\xi_i(\cdot)\}_{i=1}^n$ , while the latter reflects the influence of the variance of each observation  $Y_{ij}$  on the nonparametric smoothing, with magnitude  $J_n\mathbb{E}(N^{-1})$ . Thus, as  $n \rightarrow \infty$ , the phase transition in our framework depends on the trade-off between  $\mathbf{B}^\top(x)\boldsymbol{\Sigma}_1\mathbf{B}(x')$  and  $\mathbf{B}^\top(x)\boldsymbol{\Sigma}_2\mathbf{B}(x')$  by comparing the order of  $J_n$  and  $\mathbb{E}^{-1}(N^{-1})$ , as discussed in Assumption (A6). However, phase transition results are typically expressed in terms of the relationship between the sample size and the sampling frequency in existing literature (Zhang and Wang (2016), Zhang and Li (2022)), as this offers a more intuitive understanding. Following the idea in Cai and Hu (2024a), we first specify the relationship among  $J_n$ ,  $n$ , and  $\mathbb{E}(N^{-1})$ , and then translate the relationship between  $J_n$  and  $\mathbb{E}(N^{-1})$  into one between  $n$  and  $\mathbb{E}(N^{-1})$ . Hence, the phase transitions can be concluded as the following corollary.

**Corollary 3.1.** *Suppose that the null hypothesis  $H_0$  holds, as  $n \rightarrow \infty$ ,*

- (i) *Under Assumptions (A1)-(A6), when  $\mathbb{E}^{-1}(N^{-1}) \ll n^{1/(2q^*)} \log^{b-(2q^*+1)/q^*} n$  and  $J_n \asymp \{n\mathbb{E}^{-1}(N^{-1}) \log^{2q^*b} n\}^{1/(2q^*+1)}$  for some  $b > 1/(2q^*)$ ,*

$$\sup_{z \in \mathbb{R}} \left| \mathbb{P}(T_n \leq z) - \mathbb{P} \left( \sup_{\epsilon \leq t \leq 1-\epsilon} \sup_{x \in [0,1]} \frac{|\mathcal{Z}_{2n}(t, x)|}{\sqrt{\mathbf{B}^\top(x) \boldsymbol{\Sigma}_2 \mathbf{B}(x)}} \leq z \right) \right| \rightarrow 0. \quad (3.3)$$

- (ii) *Under Assumptions (A1)-(A6), when  $n^{1/(2q^*)} \log^{b-(2q^*+1)/q^*} n \ll \mathbb{E}^{-1}(N^{-1}) \ll n^{1/(2q^*)} \log^{1/(2q^*)+2} n$  and  $J_n \asymp n^{1/(2q^*)} \log^b n$  for some  $b > 1/(2q^*)$ , (3.1) holds.*

- (iii) *Under Assumptions (A1)-(A6), when  $\mathbb{E}^{-1}(N^{-1}) \gg n^{1/(2q^*)} \log^{1/(2q^*)+2} n$  and  $n^{1/(2q^*)} \log^{1/(2q^*)} n \ll J_n \ll \mathbb{E}^{-1}(N^{-1}) \log^{-2} n$ ,*

$$\sup_{z \in \mathbb{R}} \left| \mathbb{P}(T_n \leq z) - \mathbb{P} \left( \sup_{\epsilon \leq t \leq 1-\epsilon} \sup_{x \in [0,1]} \frac{|\mathcal{Z}_{1n}(t, x)|}{\sqrt{\mathbf{B}^\top(x) \boldsymbol{\Sigma}_1 \mathbf{B}(x)}} \leq z \right) \right| \rightarrow 0. \quad (3.4)$$

- (i') *Under Assumptions (A1)-(A5) and (A6'), when  $\mathbb{E}^{-1}(N^{-1}) \ll n^{1/(2q^*)} \log^{1/(2q^*)} n$  and  $J_n \asymp \{n\mathbb{E}^{-1}(N^{-1}) \log n\}^{1/(2q^*+1)}$ ,*

$$\sup_{z \in \mathbb{R}} \left| \mathbb{P}(S_n \leq z) - \mathbb{P} \left( \sup_{\epsilon \leq t \leq 1-\epsilon} \int_0^1 \frac{\mathcal{Z}_{2n}^2(t, x)}{\mathbf{B}^\top(x) \boldsymbol{\Sigma}_2 \mathbf{B}(x)} dx \leq z \right) \right| \rightarrow 0. \quad (3.5)$$

- (ii') *Under Assumptions (A1)-(A5) and (A6'), when  $\mathbb{E}^{-1}(N^{-1}) \asymp n^{1/(2q^*)} \log^{1/(2q^*)} n$  and  $J_n \asymp n^{1/(2q^*)} \log^{1/(2q^*)} n$ , (3.2) holds.*

- (iii') *Under Assumptions (A1)-(A5) and (A6'), when  $\mathbb{E}^{-1}(N^{-1}) \gg n^{1/(2q^*)} \log^{1/(2q^*)} n$  and  $n^{1/(2q^*)} \log^{1/(2q^*)} n \ll J_n \ll \mathbb{E}^{-1}(N^{-1})$ ,*

$$\sup_{z \in \mathbb{R}} \left| \mathbb{P}(S_n \leq z) - \mathbb{P} \left( \sup_{\epsilon \leq t \leq 1-\epsilon} \int_0^1 \frac{\mathcal{Z}_{1n}^2(t, x)}{\mathbf{B}^\top(x) \boldsymbol{\Sigma}_1 \mathbf{B}(x)} dx \leq z \right) \right| \rightarrow 0. \quad (3.6)$$

To better illustrate the intuition of this result, we ignore logarithmic factors for simplicity and call  $\sqrt{n/\mathbf{B}^\top(\cdot) \boldsymbol{\Sigma} \mathbf{B}(\cdot)}$  as the rescaling function of the proposed smoothed CUMSUM process. Overall, different leading terms in asymptotic covariance functions lead to different



approximating Gaussian processes. Specifically, when  $\mathbb{E}^{-1}(N^{-1}) \ll n^{1/(2q^*)}$ , it is referred to as the sparse scenario, where  $\mathbf{B}^\top(\cdot)\boldsymbol{\Sigma}_1\mathbf{B}(\cdot) \ll \mathbf{B}^\top(\cdot)\boldsymbol{\Sigma}_2\mathbf{B}(\cdot)$ . Due to fewer observations along each curve, the influence of the variance of each  $Y_{ij}$  dominates, and the magnitude of the rescaling function corresponds to the convergence rate of classical nonparametric regression. When  $\mathbb{E}^{-1}(N^{-1}) \gg n^{1/(2q^*)}$ , it is referred to as the dense scenario, where  $\mathbf{B}^\top(\cdot)\boldsymbol{\Sigma}_1\mathbf{B}(\cdot) \gg \mathbf{B}^\top(\cdot)\boldsymbol{\Sigma}_2\mathbf{B}(\cdot)$ . In this case, due to the sufficient number of observations on each curve, the dependency between  $\xi_i(X_{ij})$ 's dominates, with the magnitude of the rescaling function being consistent with the parametric convergence rate of  $n^{1/2}$ . When  $\mathbb{E}^{-1}(N^{-1}) \asymp n^{1/(2q^*)}$ , it is referred to as the semi-dense scenario, where the two types of effects are mixed under this intermediate regime, similar to the findings in Berger et al. (2023). The result of dense scenario also coincides with the fact that the test statistics in (2.1), (2.2) and (2.3) all enjoy parametric convergence rate of order  $n^{1/2}$  when the sampling frequency is dense.

Next, we discuss the asymptotic properties under alternative hypothesis. Consider local alternatives  $H_{1n} : \Delta_n \neq 0$ ,  $\|\Delta_n\| \rightarrow 0$ , where  $\|\cdot\|$  is sup-norm or  $\mathcal{L}_2$ -norm. Define  $\varrho_\tau(t) = t(1 - \tau)$  if  $t \leq \tau$ ,  $\tau(1 - t)$  if  $t > \tau$  and  $\tau_0 = \lim_{n \rightarrow \infty} k_0/n$ .

**Theorem 3.2.** *Suppose that the alternative hypothesis  $H_1$  holds, as  $n \rightarrow \infty$ ,*

(a) *Under Assumptions (A1)-(A6), when  $\|\Delta_n\|_\infty \lesssim \max \left\{ \sqrt{n^{-1} \log n}, \sqrt{n^{-1} \mathbb{E}(N^{-1}) J_n \log n} \right\}$ ,*

$$\sup_{z \in \mathbb{R}} \left| \mathbb{P}(T_n \leq z) - \mathbb{P} \left( \sup_{\epsilon \leq t \leq 1-\epsilon} \sup_{x \in [0,1]} \frac{|\mathcal{Z}_n(t, x) + \sqrt{n} \varrho_{\tau_0}(t) \Delta_n(x)|}{\sqrt{\mathbf{B}^\top(x) \boldsymbol{\Sigma} \mathbf{B}(x)}} \leq z \right) \right| \rightarrow 0. \quad (3.7)$$

*For any  $\alpha \in (0, 1)$ , when  $\|\Delta_n\|_\infty \gtrsim \max \left\{ \sqrt{n^{-1} \log n}, \sqrt{n^{-1} \mathbb{E}(N^{-1}) J_n \log n} \right\}$ ,  $\mathbb{P}(T_n > Q_{T_n, 1-\alpha}) > \alpha$ ; when  $\|\Delta_n\|_\infty \gg \max \left\{ \sqrt{n^{-1} \log n}, \sqrt{n^{-1} \mathbb{E}(N^{-1}) J_n \log n} \right\}$ ,  $\mathbb{P}(T_n > Q_{T_n, 1-\alpha}) \rightarrow 1$ .*

(b) *Under Assumptions (A1)-(A5), (A6'), when  $\|\Delta_n\|_{\mathcal{L}_2} \lesssim \max \left\{ \sqrt{n^{-1}}, \sqrt{n^{-1} \mathbb{E}(N^{-1}) J_n} \right\}$ ,*

$$\sup_{z \in \mathbb{R}} \left| \mathbb{P}(S_n \leq z) - \mathbb{P} \left( \sup_{\epsilon \leq t \leq 1-\epsilon} \int_0^1 \frac{|\mathcal{Z}_n(t, x) + \sqrt{n} \varrho_{\tau_0}(t) \Delta_n(x)|^2}{\mathbf{B}^\top(x) \boldsymbol{\Sigma} \mathbf{B}(x)} dx \leq z \right) \right|. \quad (3.8)$$

For any  $\alpha \in (0, 1)$ , when  $\|\Delta_n\|_{\mathcal{L}_2} \gtrsim \max \left\{ \sqrt{n^{-1}}, \sqrt{n^{-1}\mathbb{E}(N^{-1})J_n} \right\}$ ,  $\mathbb{P}(S_n > Q_{S_n, 1-\alpha}) > \alpha$ ; when  $\|\Delta_n\|_{\mathcal{L}_2} \gg \max \left\{ \sqrt{n^{-1}}, \sqrt{n^{-1}\mathbb{E}(N^{-1})J_n} \right\}$ ,  $\mathbb{P}(S_n > Q_{S_n, 1-\alpha}) \rightarrow 1$ .

For any  $\alpha \in (0, 1)$ , the  $\alpha$ -quantiles  $Q_{T_n, \alpha}$ ,  $Q_{S_n, \alpha}$  are defined by

$$\mathbb{P} \left( \sup_{\epsilon \leq t \leq 1-\epsilon} \sup_{x \in [0, 1]} \frac{|\mathcal{Z}_n(t, x)|}{\sqrt{\mathbf{B}^\top(x) \boldsymbol{\Sigma} \mathbf{B}(x)}} \leq Q_{T_n, \alpha} \right) = \mathbb{P} \left( \sup_{\epsilon \leq t \leq 1-\epsilon} \int_0^1 \frac{\mathcal{Z}_n^2(t, x)}{\mathbf{B}^\top(x) \boldsymbol{\Sigma} \mathbf{B}(x)} dx \leq Q_{S_n, \alpha} \right) = \alpha.$$

Theorem 3.2 provides meticulous power analysis of  $T_n$  and  $S_n$  under the local alternatives. To avoid redundancy, we take  $S_n$  as an example. Under dense or semi-dense scenarios that  $\mathbb{E}(N^{-1})J_n \lesssim 1$ , the test has nontrivial power when the jump magnitude exceeds an order of  $n^{-1/2}$ ; while under sparse scenarios that  $\mathbb{E}(N^{-1})J_n \gg 1$ , the test has nontrivial power when the jump magnitude exceeds an order of  $\mathbb{E}^{1/2}(N^{-1})J_n^{1/2}n^{-1/2}$ . Therefore, for testing the hypothesis in (1.2), Theorems (3.1) and (3.2) show that the decision rules  $T_n \geq Q_{T_n, 1-\alpha}$  and  $S_n \geq Q_{S_n, 1-\alpha}$  are consistent with significance level  $\alpha$ .

Furthermore, according to Theorem 3.2, it is interesting to note that the  $\mathcal{L}_2$ -based test statistic  $S_n$  theoretically has a better power than the  $\mathcal{L}_\infty$ -based statistic  $T_n$ . However, our simulation experiments indicate that the empirical performance of  $T_n$  might surpass that of  $S_n$  with finite sample sizes, especially when the jump function exhibits sharp peaks.

## 3.2 Asymptotic properties of break point estimators

Next, we investigate the convergence rate of the proposed break point estimators.

**Theorem 3.3.** *Under Assumptions (A1)-(A5),  $nJ_n^{-q^*} = o(1 + J_n\mathbb{E}(N^{-1}))$ ,  $n^{-1/2}J_n \log(n) = o(1)$ , and  $\|\Delta\|_{\mathcal{L}_2} > 0$ ,  $|\widehat{k}_{n,2} - k_0| = \mathcal{O}_p(\max\{1, J_n\mathbb{E}(N^{-1})\})$ . Under Assumptions (A1)-(A6) and  $\|\Delta\|_{\mathcal{L}_\infty} > 0$ ,  $|\widehat{k}_{n,\infty} - k_0| = \mathcal{O}_p\left(n^{1/2} \log^{1/2}(n) \max\left\{1, J_n^{1/2}\mathbb{E}^{1/2}(N^{-1})\right\}\right)$ .*

Firstly, the convergence rate of  $\widehat{k}_{n,2}$  in Theorem 3.3 is optimal for the dense case where  $\mathbb{E}(N^{-1}) \lesssim J_n$ , as the asymptotic distribution of the estimator for  $\widehat{k}_{n,2}$  has been established

in Aue et al. (2018) for fully observed trajectories, implying that  $\widehat{k}_{n,2} - k_0$  weakly converges to some non-degenerate random variable. Secondly, leveraging the relationship among  $J_n$ ,  $n$ , and  $\mathbb{E}(N^{-1})$  in Corollary 3.1, the convergence rate of  $\widehat{k}_{n,2}$  is faster by some logarithmic order compared to the detector developed in Madrid Padilla et al. (2022) from sparse to dense. Lastly, although the convergence rate of  $\widehat{k}_{n,\infty}$  is sub-optimal, which is an artifact of the proof technique due to the absence of an inner product in the Banach space  $C[0, 1]$ , we empirically find that  $\widehat{k}_{n,\infty}$  becomes more accurate than  $\widehat{k}_{n,\infty}$  with finite sample sizes when the jump function shows sharp spikes, as shown in Figure 2.

### 3.3 Inference for the jump magnitude

Given an estimation  $\widehat{k}_n$  of break point, we then aim to conduct simultaneous inference for the jump magnitude  $\Delta(\cdot)$ , while inference for the mean functions before and after the true break point  $k_0$  follows a similar approach. Note that  $\widehat{k}_n$  can be specified by users. Our proposed estimator  $\widehat{k}_{n,2}$  in (2.9) is a default choice, but any consistent estimator that satisfies the following assumption can be used.

(B1) The estimator of the break point satisfies that

$$\left| \widehat{k}_n - k_0 \right| = \mathcal{O}_p \left( \max \left\{ n^{1/2} \log^{-1/2} n, n^{1/2} J_n^{1/2} \mathbb{E}^{1/2}(N^{-1}) \log^{-1/2} n \right\} \right).$$

**Theorem 3.4.** *Suppose that the alternative hypothesis  $H_1$  holds with  $\tau_0 \in [\epsilon, 1 - \epsilon]$  for some  $\epsilon \in (0, 1/2)$ . Under Assumptions (A1)-(A6) and there exist Gaussian processes  $\mathcal{N}_n(x)$ 's with mean zero and covariance function  $\text{Cov}(\mathcal{N}_n(x), \mathcal{N}_n(x')) = \mathbf{B}^\top(x) \boldsymbol{\Sigma} \mathbf{B}(x')$ , such that*

$$\sup_{z \in \mathbb{R}} \left| \mathbb{P} \left( \left\| \frac{\sqrt{n \{ \tau_0(1 - \tau_0) \}} \left\{ \widehat{\Delta}_n(\cdot) - \Delta(\cdot) \right\}}{\sqrt{\mathbf{B}^\top(\cdot) \boldsymbol{\Sigma} \mathbf{B}(\cdot)}} \right\|_\infty \leq z \right) - \mathbb{P} \left( \left\| \frac{\mathcal{N}_n(\cdot)}{\sqrt{\mathbf{B}^\top(\cdot) \boldsymbol{\Sigma} \mathbf{B}(\cdot)}} \right\|_\infty \leq z \right) \right| \rightarrow 0.$$

Theorem 3.4 establishes Gaussian approximation for the jump estimator  $\widehat{\Delta}_n(\cdot)$  in (2.10), valid for both sparse and dense functional time series data, which shed lights on constructing

an asymptotically correct SCB with varying width for the jump magnitude. Furthermore, one could easily establish the corresponding phase transition results, similar to those in Corollary 3.1, but omit them for brevity.

## 4 Implementation

### 4.1 Testing the break point

Given the estimation of the break point  $\widehat{k}_n$ , one computes residuals  $\widehat{U}_{ij} = \{Y_{ij} - \widehat{m}_{\widehat{k}_n}(X_{ij})\} \mathbf{1}_{\{i \leq \widehat{k}_n\}} + \{Y_{ij} - \widehat{m}_{\widehat{k}_n+1}(X_{ij})\} \mathbf{1}_{\{i > \widehat{k}_n\}}$ . Define  $\widehat{\Sigma}_1 = \sum_{h=-L}^L \widehat{\Sigma}_{1,h}$ , and

$$\widehat{\Sigma}_2 = \widehat{\mathbf{V}}^{-1} \left[ \frac{1}{n} \sum_{i=1}^n \frac{1}{N_i} \sum_{j=1}^{N_i} \mathbf{B}(X_{ij}) \mathbf{B}^\top(X_{ij}) \left\{ \widehat{U}_{ij}^2 + \sum_{h=-L, h \neq 0}^L \mathbf{B}^\top(X_{ij}) \widehat{\Sigma}_{1,h} \mathbf{B}(X_{ij}) \right\} \right] \widehat{\mathbf{V}}^{-1},$$

where

$$\begin{aligned} \widehat{\Sigma}_{1,h} &= \widehat{\mathbf{V}}^{-1} \left\{ \frac{1}{n} \sum_{i=1}^{n-h} \frac{1}{N_i N_{i+h}} \sum_{j=1}^{N_i} \sum_{j'=1}^{N_{i+h}} \mathbf{B}(X_{ij}) \mathbf{B}^\top(X_{i+h,j'}) \widehat{U}_{ij} \widehat{U}_{i+h,j'} \right\} \widehat{\mathbf{V}}^{-1}, \\ \widehat{\Sigma}_{1,0} &= \widehat{\mathbf{V}}^{-1} \left\{ \frac{1}{n} \sum_{i=1}^n \frac{1}{N_i(N_i-1)} \sum_{j \neq j'}^{N_i} \mathbf{B}(X_{ij}) \mathbf{B}^\top(X_{ij'}) \widehat{U}_{ij} \widehat{U}_{ij'} \right\} \widehat{\mathbf{V}}^{-1}, \end{aligned}$$

and  $L = L(n)$  diverges as  $n$  goes to infinity. Based on the empirical guidelines from Li et al. (2023) and Hu and Li (2024), we consider values of  $L = [n^{1/5}], \dots, [n^{1/5} \log \log n]$  in the numerical simulations. The numerical results were similar across these values, and we ultimately choose  $L = [n^{1/5}]$  as the default. For the regular fixed design setting where  $X_{ij} \equiv j/N$  and  $N_i \equiv N$  for all  $i = 1, \dots, n$ , one could adopt the following simplified estimator of  $\Sigma_2$ ,

$$\widetilde{\Sigma}_2 = \widehat{\mathbf{V}}^{-1} \left\{ \frac{1}{nN} \sum_{j=1}^N \mathbf{B}(j/N) \mathbf{B}^\top(j/N) \sum_{h=-L}^L \sum_{i=1}^n \widehat{U}_{ij} \widehat{U}_{i+h,j} \right\} \widehat{\mathbf{V}}^{-1}.$$

To obtain the critical values of the proposed  $\mathcal{L}_2$  test and  $\mathcal{L}_\infty$  test from sparse to dense, it suffices to obtain the quantile of the maximum value of the Gaussian process

$\int_0^1 \{\mathbf{B}^\top(x)\boldsymbol{\Sigma}\mathbf{B}(x)\}^{-1}\mathcal{Z}_n^2(\cdot, x)dx$  and the Gaussian field  $\{\mathbf{B}^\top(\cdot)\boldsymbol{\Sigma}\mathbf{B}(\cdot)\}^{-1/2}|\mathcal{Z}_n(\star, \cdot)|$ , on  $[\epsilon, 1-\epsilon]$  and  $[\epsilon, 1-\epsilon] \times [0, 1]$  respectively, which is vital to generate Gaussian process with mean zero, whose covariance structure mimics that of  $\int_0^1 \{\mathbf{B}^\top(x)\boldsymbol{\Sigma}\mathbf{B}(x)\}^{-1}\mathcal{Z}_n^2(\cdot, x)dx$  and  $\{\mathbf{B}^\top(\cdot)\boldsymbol{\Sigma}\mathbf{B}(\cdot)\}^{-1/2}|\mathcal{Z}_n(\star, \cdot)|$  by the plug-in principle. The following outlines an efficient computation method. Given the data  $\{X_{ij}, Y_{ij}\}_{i=1, j=1}^{n, N_i}$ , one first computes the eigenvalues and eigenfunctions of covariance function  $\{\mathbf{B}^\top(\star)\widehat{\boldsymbol{\Sigma}}\mathbf{B}(\star)\}^{-1/2}\{\mathbf{B}^\top(\star)\widehat{\boldsymbol{\Sigma}}\mathbf{B}(\cdot)\}\{\mathbf{B}^\top(\cdot)\widehat{\boldsymbol{\Sigma}}\mathbf{B}(\cdot)\}^{-1/2}$ , denoted by  $\{\widehat{\vartheta}_{kn}, \widehat{\varphi}_{kn}(\cdot)\}_{k=1}^{N_s+p}$ . Let  $\widehat{\kappa} = \arg \min_{1 \leq v \leq T} \left\{ \sum_{k=1}^v \widehat{\vartheta}_k / \sum_{k=1}^T \widehat{\vartheta}_k > 0.99 \right\}$ , where  $\{\widehat{\vartheta}_k\}_{k=1}^T$  are the first  $T$  estimated positive eigenvalues. Then, one generates i.i.d. Brownian bridges  $\{\mathcal{B}_{b,k}(\cdot)\}_{b,k=1}^{B, \widehat{\kappa}}$ , and defines  $\Xi_{b,n}(t) = \sum_{k=1}^{\widehat{\kappa}} \widehat{\vartheta}_k \mathcal{B}_{b,k}^2(t)$ ,  $\Upsilon_{b,n}(t, x) = \sum_{k=1}^{\widehat{\kappa}} \widehat{\vartheta}_k^{1/2} \widehat{\varphi}_k(x) \mathcal{B}_{b,k}(t)$ . Denote by  $\widehat{Q}_{S_n, \alpha}$ ,  $\widehat{Q}_{T_n, \alpha}$  the empirical upper- $\alpha$  quantile of the maximal absolute value for  $\{\Xi_{b,n}(\cdot)\}_{b=1}^B$  and  $\{\Upsilon_{b,n}(\star, \cdot)\}_{b=1}^B$ , respectively. Define

$$\widehat{T}_n = \sup_{\epsilon \leq t \leq 1-\epsilon} \left\| \frac{[nt]\widehat{m}(t, \cdot)/\sqrt{n} - \sqrt{nt}\widehat{m}(\cdot)}{\sqrt{\mathbf{B}^\top(\cdot)\widehat{\boldsymbol{\Sigma}}\mathbf{B}(\cdot)}} \right\|_{\infty}, \quad \widehat{S}_n = \sup_{\epsilon \leq t \leq 1-\epsilon} \left\| \frac{[nt]\widehat{m}(t, \cdot)/\sqrt{n} - \sqrt{nt}\widehat{m}(\cdot)}{\sqrt{\mathbf{B}^\top(\cdot)\widehat{\boldsymbol{\Sigma}}\mathbf{B}(\cdot)}} \right\|_{\mathcal{L}_2}^2.$$

Hence, an  $\mathcal{L}_2$  ( $\mathcal{L}_\infty$ ) test of significance level  $\alpha$  rejects the null  $H_0$  in (1.2) if  $\widehat{S}_n > \widehat{Q}_{S_n, \alpha}$  ( $\widehat{T}_n > \widehat{Q}_{T_n, \alpha}$ ).

## 4.2 Simultaneous confidence bands of the jump

To construct the simultaneous confidence band of the jump magnitude  $\Delta(\cdot)$ , it suffices to obtain the quantile of the sup-norm of the Gaussian process  $\{\mathbf{B}^\top(\cdot)\boldsymbol{\Sigma}\mathbf{B}(\cdot)\}^{-1/2}|\mathcal{N}_n(\cdot)|$ . To obtain the estimated quantile, it is crucial to generate a Gaussian process with a mean of zero, whose covariance structure emulates that of  $\{\mathbf{B}^\top(\cdot)\boldsymbol{\Sigma}\mathbf{B}(\cdot)\}^{-1/2}|\mathcal{N}_n(\cdot)|$  using the plug-in principle. One generates i.i.d.  $(J_n + p)$ -dimensional Gaussian random vectors  $\{\mathbf{Z}_{b,n}\}_{b=1}^B$  with mean zero and covariance matrix  $\widehat{\boldsymbol{\Sigma}}$ , independent of the data  $\{X_{ij}, Y_{ij}\}_{i=1, j=1}^{n, N_i}$ , and calculate the empirical upper- $\alpha$  quantile of the maximal absolute value

for  $\{\{\mathbf{B}^\top(\cdot)\widehat{\Sigma}\mathbf{B}(\cdot)\}^{-1/2}\mathbf{B}^\top(\cdot)\mathbf{Z}_{b,n}\}_{b=1}^B$ , denoted by  $\widehat{Q}_{\Delta,\alpha}$ . An asymptotic  $100(1-\alpha)\%$  SCB for  $\Delta(x)$  over  $x \in [0, 1]$  is given by  $\widehat{\Delta}_n(x) \pm n^{-1/2}\{\mathbf{B}^\top(\cdot)\widehat{\Sigma}\mathbf{B}(\cdot)\}^{1/2}\widehat{Q}_{\Delta,\alpha}$ ,  $x \in [0, 1]$ .

## 5 Numerical simulation

### 5.1 General settings

A total of four sampling schemes from sparse to dense are taken into consideration.  $N_i$  are i.i.d. from a discrete uniform distribution on the set, (1)  $\{3, 4, 5, 6\}$ , (2)  $\{\lfloor 2n^{1/5} \rfloor, \lfloor 2n^{1/5} \rfloor + 1, \dots, \lfloor 4n^{1/5} \rfloor\}$ , (3)  $\{\lfloor n^{1/2} \rfloor, \lfloor n^{1/2} \rfloor + 1, \dots, \lfloor 2n^{1/2} \rfloor\}$ , and (4)  $\{\lfloor n/8 \rfloor, \lfloor n/8 \rfloor + 1, \dots, \lfloor n/4 \rfloor\}$ . We also evaluate three types of the jump function, (i)  $\Delta_a(x) \equiv a$ , (ii)  $\Delta_a(x) \equiv 4\sqrt{5}a(x - 1/2)^2$ , (iii)  $\Delta_a(x) = a * \sqrt{\beta_{10,1000}(x) + \beta_{1000,1000}(x) + \beta_{1000,10}(x)}/\sqrt{3}$ , in which  $\beta_{a,b}(x)$  is the probability density function of  $\beta$ -distribution, each satisfying that  $\|\Delta_a\|_{\mathcal{L}_2} = a$ . We consider  $a = 0, 0.2, 0.4, \dots, 1$ , where  $a = 0$  represents the null hypothesis, and  $a > 0$  represents the alternative hypothesis in (1.2).

According to the Karhunen-Loève representation (Hsing and Eubank (2015)), the data are generated from the following model (5.1) by rewriting model (1.1) as

$$Y_{ij} = m(X_{ij}) + \sum_{k=1}^{\infty} \sqrt{\lambda_k} \xi_{ik} \psi_k(X_{ij}) + \sigma(X_{ij}) \epsilon_{ij}, \quad 1 \leq i \leq n, \quad 1 \leq j \leq N_i. \quad (5.1)$$

Here, the eigenvalues  $\lambda_1 \geq \lambda_2 \geq \dots \geq 0$  satisfying  $\sum_{k=1}^{\infty} \lambda_k < \infty$ , and the corresponding eigenfunctions  $\{\psi_k\}_{k=1}^{\infty}$  form an orthonormal basis of  $\mathcal{L}^2[0, 1]$ . The random coefficients  $\{\xi_{ik}\}_{k=1}^{\infty}$ , called FPC scores, are uncorrelated with mean 0 and variance 1. In each case, we set  $m_1(x) = \dots = m_{k_0}(x) = 3/2 \sin\{3\pi(x+1/2)\} + 2x^3$ ,  $m_{k_0+1}(x) = \dots = m_n(x) = m_{k_0}(x) + \Delta_a(x)$  for  $a = 0, 0.2, 0.4, \dots, 1$ , and  $\lambda_k = 2^{1-k}$  for  $k = 1, \dots, 4$  and  $\lambda_k = 0$  for  $k \geq 5$ ,  $\psi_{2k-1} = \sqrt{2} \sin(2k\pi x)$  and  $\psi_{2k} = \sqrt{2} \cos(2k\pi x)$  for  $k \in \mathbb{Z}_+$ . Besides, the FPC scores  $\{\xi_{tk}\}_{t=1, k=1}^{n, 4}$  are generated from the MA(1) process,  $\xi_{tk} = 0.8\zeta_{tk} + 0.6\zeta_{t-1, k}$ , where  $\{\zeta_{tk}\}_{t=0, k=1}^{n, 2}$  are i.i.d.

random variables, and  $X_{ij}$ 's are independently generated from the uniform distribution  $U(0, 1)$ . The measurement errors  $\varepsilon_{ij}$ 's are i.i.d. standard normal random variables, with the variance function  $\sigma^2(x) \equiv 1$ . We consider different distributions of the FPC scores, including the standard normal distribution  $N(0, 1)$ , the uniform distribution  $U(-\sqrt{3}, \sqrt{3})$ , and the standardized Laplace distribution with density  $f(x) = 2^{-1/2} \exp(\sqrt{2}|x|)$ . The number of sample size  $n$  is set at 200 and 400. The empirical replications  $B$  in the quantile estimation and the Monte Carlo replications are both 500.

The cubic splines with  $p = 4$  are used in our numerical simulations. Besides, the number  $J_n$  of interior knots is an important smoothing parameter, and we recommend using a data-driven procedure to select  $J_n \in [\min\{0.5(n\bar{N})^{1/9}, 0.5n^{1/8}\}, \max\{(n\bar{N})^{1/7}, n^{1/6}\}]$  by minimizing the following BIC criterion:

$$\begin{aligned} \text{BIC}(J_n) = \log & \left( \frac{1}{n} \sum_{i=1}^n \frac{1}{N_i} \sum_{j=1}^{N_i} \left[ \left\{ Y_{ij} - \widehat{m}_{\widehat{k}_{n,2}, J_n}(X_{ij}) \right\}^2 \mathbf{1} \{i \leq \widehat{k}_{n,2}\} \right. \right. \\ & \left. \left. + \left\{ Y_{ij} - \widehat{m}_{\widehat{k}_{n,2}+1, J_n}(X_{ij}) \right\}^2 \mathbf{1} \{i > \widehat{k}_{n,2}\} \right] \right) + \frac{(J_n + p) \log(n)}{n}, \end{aligned}$$

where  $\widehat{k}_{n,2}$ ,  $\widehat{m}_{\widehat{k}_{n,2}, J_n}(\cdot)$  and  $\widehat{m}_{\widehat{k}_{n,2}+1, J_n}(\cdot)$  are defined in (2.9), (2.11) and (2.12) respectively, with the number  $J_n$  of interior knots.

## 5.2 Size and power examination

From Tables 1-2, we have the following findings. First, the empirical size of our developed testing procedure is generally close to the predetermined significance level  $\alpha = 0.05$ . Besides, as the strength of the jump signal (i.e., the value of  $a$ ) increases, the empirical power of the proposed tests improves. Moreover, the empirical size and power of the tests are insensitive to the distribution of the stochastic process  $\xi_i(\cdot)$ .

Furthermore, regarding the power under the alternative hypothesis, the  $\mathcal{L}_\infty$  statistic  $T_n$  tends to exhibit superior performance when the sampling frequency is dense and the jump

magnitudes are sharper, particularly for Type (iii) jump. In contrast, the  $\mathcal{L}_2$  statistic  $S_n$  is more effective under sparser sampling frequencies and flatter jump functions, especially for Type (i) jump.

### 5.3 SCB of jump magnitudes

To assess the proposed inference procedure of jumps, we only consider two types (i) and (ii), which are generally smooth. Tables 3 show that in each case, the empirical coverage rates of the proposed SCRs are close to the nominal confidence level  $1 - \alpha$ , a positive confirmation of the asymptotic theory.

## 6 Application

### 6.1 Electricity price-versus-demand data

We adopt the proposed methods to analyze the daily price-versus-demand curves of the German electricity power market in 2011. The data set records the hourly gross electricity demand in Germany  $\{X_{ij}\}_{i,j=1}^{n,N_i}$  and the average hourly electricity prices  $\{Y_{ij}\}_{i,j=1}^{n,N_i}$ , and is available from Supplement B of Liebl (2019). Similar datasets from different years have attracted much interest from statisticians and have been extensively studied in the literature; see Liebl (2013), Liebl (2019), Kneip and Liebl (2020) and Xue et al. (2024) for instance.

After removing missing data points, we construct the model in (1.1) by pairing electricity demand with electricity prices based on their timestamps to form a single data point, then treating the data points from each day as observations of a realization of a stochastic process. Then, the sample size and the number of observations in each trajectory are given



Jump	FPC score/ $a$	$\mathcal{L}_2$						$\mathcal{L}_\infty$					
		0	0.2	0.4	0.6	0.8	1	0	0.2	0.4	0.6	0.8	1
Setting (1)													
Type (i)	Normal	0.044	0.156	0.586	0.964	1.000	1.000	0.056	0.212	0.498	0.826	0.972	0.998
	Uniform	0.050	0.166	0.564	0.952	1.000	1.000	0.072	0.158	0.478	0.826	0.976	0.998
	Laplace	0.076	0.144	0.606	0.960	1.000	1.000	0.086	0.194	0.474	0.806	0.986	1.000
Type (ii)	Normal	0.054	0.132	0.368	0.810	0.992	1.000	0.070	0.160	0.582	0.896	0.996	1.000
	Uniform	0.056	0.112	0.358	0.806	0.990	1.000	0.070	0.188	0.556	0.892	0.996	1.000
	Laplace	0.072	0.118	0.370	0.824	0.994	1.000	0.080	0.196	0.578	0.910	0.994	1.000
Type (iii)	Normal	0.054	0.086	0.120	0.256	0.482	0.652	0.074	0.234	0.344	0.516	0.694	0.790
	Uniform	0.064	0.086	0.172	0.338	0.456	0.692	0.076	0.224	0.390	0.546	0.676	0.818
	Laplace	0.064	0.088	0.160	0.306	0.500	0.674	0.076	0.230	0.370	0.548	0.736	0.812
Setting (2)													
Type (i)	Normal	0.054	0.154	0.712	0.992	1.000	1.000	0.054	0.222	0.564	0.936	1.000	1.000
	Uniform	0.060	0.166	0.688	0.998	1.000	1.000	0.066	0.208	0.588	0.908	0.998	1.000
	Laplace	0.056	0.172	0.702	0.996	1.000	1.000	0.054	0.186	0.578	0.942	1.000	1.000
Type (ii)	Normal	0.060	0.126	0.464	0.930	1.000	1.000	0.070	0.224	0.718	0.964	0.998	1.000
	Uniform	0.062	0.104	0.458	0.946	1.000	1.000	0.066	0.204	0.714	0.972	1.000	1.000
	Laplace	0.064	0.092	0.470	0.948	1.000	1.000	0.050	0.214	0.728	0.980	1.000	1.000
Type (iii)	Normal	0.072	0.084	0.124	0.282	0.618	0.820	0.072	0.156	0.414	0.608	0.846	0.918
	Uniform	0.058	0.088	0.152	0.300	0.556	0.816	0.066	0.148	0.390	0.632	0.816	0.942
	Laplace	0.054	0.072	0.168	0.308	0.608	0.832	0.066	0.162	0.370	0.642	0.844	0.936
Setting (3)													
Type (i)	Normal	0.076	0.164	0.910	1.000	1.000	1.000	0.074	0.246	0.764	0.992	1.000	1.000
	Uniform	0.066	0.168	0.906	1.000	1.000	1.000	0.066	0.270	0.766	0.998	1.000	1.000
	Laplace	0.074	0.170	0.886	1.000	1.000	1.000	0.058	0.248	0.792	0.996	1.000	1.000
Type (ii)	Normal	0.074	0.122	0.646	0.994	1.000	1.000	0.076	0.310	0.876	1.000	1.000	1.000
	Uniform	0.072	0.146	0.654	1.000	1.000	1.000	0.070	0.320	0.892	0.998	1.000	1.000
	Laplace	0.064	0.136	0.666	0.994	1.000	1.000	0.072	0.302	0.896	1.000	1.000	1.000
Type (iii)	Normal	0.062	0.068	0.154	0.436	0.836	0.978	0.064	0.196	0.590	0.900	0.996	1.000
	Uniform	0.072	0.090	0.176	0.410	0.834	0.980	0.054	0.200	0.610	0.910	0.996	1.000
	Laplace	0.070	0.076	0.142	0.470	0.818	0.972	0.056	0.202	0.602	0.930	0.990	1.000
Setting (4)													
Type (i)	Normal	0.072	0.172	0.942	1.000	1.000	1.000	0.066	0.324	0.838	1.000	1.000	1.000
	Uniform	0.064	0.172	0.942	1.000	1.000	1.000	0.076	0.288	0.824	1.000	1.000	1.000
	Laplace	0.048	0.152	0.942	1.000	1.000	1.000	0.058	0.302	0.858	1.000	1.000	1.000
Type (ii)	Normal	0.076	0.186	0.758	1.000	1.000	1.000	0.070	0.382	0.908	1.000	1.000	1.000
	Uniform	0.074	0.164	0.720	1.000	1.000	1.000	0.076	0.384	0.912	1.000	1.000	1.000
	Laplace	0.074	0.150	0.736	1.000	1.000	1.000	0.064	0.396	0.940	1.000	1.000	1.000
Type (iii)	Normal	0.068	0.090	0.170	0.558	0.944	0.996	0.072	0.262	0.734	0.984	1.000	1.000
	Uniform	0.070	0.094	0.178	0.534	0.934	0.996	0.064	0.228	0.752	0.978	1.000	1.000
	Laplace	0.058	0.082	0.184	0.506	0.934	0.998	0.066	0.284	0.752	0.980	1.000	1.000

Table 1: Empirical size and power of the proposed  $\mathcal{L}_2$  and  $\mathcal{L}_\infty$  tests with  $n = 200$ .

Jump	FPC score/a	L2						Linfinity					
		0	0.2	0.4	0.6	0.8	1	0	0.2	0.4	0.6	0.8	1
Setting (1)													
Type (i)	Normal	0.058	0.228	0.934	1.000	1.000	1.000	0.052	0.222	0.698	0.988	1.000	1.000
	Uniform	0.050	0.296	0.944	1.000	1.000	1.000	0.046	0.220	0.682	0.976	1.000	1.000
	Laplace	0.050	0.266	0.922	1.000	1.000	1.000	0.044	0.200	0.674	0.992	1.000	1.000
Type (ii)	Normal	0.044	0.148	0.750	0.996	1.000	1.000	0.052	0.264	0.844	0.992	1.000	1.000
	Uniform	0.046	0.148	0.720	0.998	1.000	1.000	0.048	0.272	0.862	1.000	1.000	1.000
	Laplace	0.044	0.124	0.730	0.994	1.000	1.000	0.058	0.272	0.848	0.998	1.000	1.000
Type (iii)	Normal	0.060	0.066	0.146	0.472	0.796	0.956	0.048	0.120	0.358	0.712	0.892	0.968
	Uniform	0.054	0.076	0.176	0.484	0.758	0.932	0.046	0.144	0.384	0.670	0.866	0.962
	Laplace	0.040	0.052	0.156	0.456	0.790	0.934	0.038	0.118	0.440	0.692	0.886	0.952
Setting (2)													
Type (i)	Normal	0.062	0.308	0.994	1.000	1.000	1.000	0.050	0.242	0.912	1.000	1.000	1.000
	Uniform	0.056	0.258	1.000	1.000	1.000	1.000	0.048	0.264	0.922	1.000	1.000	1.000
	Laplace	0.046	0.318	0.994	1.000	1.000	1.000	0.040	0.308	0.892	1.000	1.000	1.000
Type (ii)	Normal	0.066	0.176	0.926	1.000	1.000	1.000	0.044	0.330	0.970	1.000	1.000	1.000
	Uniform	0.056	0.194	0.916	1.000	1.000	1.000	0.042	0.376	0.966	1.000	1.000	1.000
	Laplace	0.052	0.176	0.922	1.000	1.000	1.000	0.050	0.348	0.958	1.000	1.000	1.000
Type (iii)	Normal	0.054	0.094	0.242	0.668	0.968	1.000	0.036	0.178	0.564	0.898	0.998	1.000
	Uniform	0.058	0.064	0.244	0.662	0.986	0.998	0.038	0.146	0.592	0.908	0.998	1.000
	Laplace	0.050	0.066	0.290	0.678	0.964	0.998	0.046	0.172	0.598	0.942	0.998	1.000
Setting (3)													
Type (i)	Normal	0.066	0.440	1.000	1.000	1.000	1.000	0.056	0.378	0.996	1.000	1.000	1.000
	Uniform	0.068	0.430	1.000	1.000	1.000	1.000	0.048	0.394	0.996	1.000	1.000	1.000
	Laplace	0.070	0.466	1.000	1.000	1.000	1.000	0.068	0.400	0.996	1.000	1.000	1.000
Type (ii)	Normal	0.060	0.292	0.998	1.000	1.000	1.000	0.052	0.624	1.000	1.000	1.000	1.000
	Uniform	0.054	0.318	0.998	1.000	1.000	1.000	0.046	0.620	0.998	1.000	1.000	1.000
	Laplace	0.068	0.288	0.998	1.000	1.000	1.000	0.058	0.624	0.998	1.000	1.000	1.000
Type (iii)	Normal	0.050	0.098	0.428	0.970	1.000	1.000	0.044	0.338	0.926	1.000	1.000	1.000
	Uniform	0.056	0.114	0.402	0.954	1.000	1.000	0.040	0.328	0.936	1.000	1.000	1.000
	Laplace	0.052	0.110	0.380	0.956	1.000	1.000	0.054	0.298	0.942	0.998	1.000	1.000
Setting (4)													
Type (i)	Normal	0.060	0.452	1.000	1.000	1.000	1.000	0.064	0.488	1.000	1.000	1.000	1.000
	Uniform	0.064	0.468	1.000	1.000	1.000	1.000	0.052	0.498	1.000	1.000	1.000	1.000
	Laplace	0.060	0.478	1.000	1.000	1.000	1.000	0.064	0.516	1.000	1.000	1.000	1.000
Type (ii)	Normal	0.058	0.322	1.000	1.000	1.000	1.000	0.066	0.724	1.000	1.000	1.000	1.000
	Uniform	0.046	0.358	1.000	1.000	1.000	1.000	0.060	0.712	1.000	1.000	1.000	1.000
	Laplace	0.062	0.366	1.000	1.000	1.000	1.000	0.064	0.726	1.000	1.000	1.000	1.000
Type (iii)	Normal	0.068	0.116	0.512	1.000	1.000	1.000	0.064	0.424	0.992	1.000	1.000	1.000
	Uniform	0.060	0.112	0.522	0.998	1.000	1.000	0.068	0.438	0.992	1.000	1.000	1.000
	Laplace	0.046	0.096	0.550	1.000	1.000	1.000	0.050	0.452	0.990	1.000	1.000	1.000

Table 2: Empirical size and power of the proposed  $\mathcal{L}_2$  and  $\mathcal{L}_\infty$  tests with  $n = 400$ .

$n$	Setting/FPC score	Type (i)			Type (ii)		
		Normal	Uniform	Laplace	Normal	Uniform	Laplace
200	Setting (1)	0.936	0.956	0.946	0.938	0.948	0.942
	Setting (2)	0.946	0.952	0.946	0.934	0.938	0.924
	Setting (3)	0.952	0.930	0.944	0.938	0.950	0.940
	Setting (4)	0.932	0.958	0.922	0.960	0.952	0.936
400	Setting (1)	0.954	0.964	0.956	0.968	0.954	0.962
	Setting (2)	0.964	0.966	0.966	0.956	0.950	0.960
	Setting (3)	0.950	0.958	0.952	0.950	0.962	0.952
	Setting (4)	0.948	0.956	0.954	0.948	0.940	0.948

Table 3: Empirical coverage rates of proposed 95% SCB for the jump magnitude( $a = 1$ ).

by  $n = 364$  and  $N_i = 24$  for  $i = 1, \dots, n$ . Firstly, we are interested in testing whether the mean function of the curve data undergoes an abrupt change. Our proposed  $\mathcal{L}_2$  and  $\mathcal{L}_\infty$  tests both strongly reject the null hypothesis, with p-values smaller than 0.001. Then, the we use the developed break point estimators  $\hat{k}_{n,2}$  and  $\hat{k}_{n,\infty}$  to locate the break point. Interestingly, both estimators identified the break point  $n = 74$  as March 15, 2011. This can be explained as the result of the Fukushima nuclear leak in Japan on March 11, 2011. After the Fukushima incident, Germany permanently shut down 40% of its nuclear power plants on March 15, leading to significant price fluctuations in the electricity market. The reduction in nuclear power generation caused a tightening of electricity supply, resulting in a short-term increase in electricity prices, as similar results emphasized in Liebl (2019).

The left panel in Figure 3 shows the electricity price-demand curves before and after March 15, along with the estimated mean curves, further confirming the abrupt rise in Germany's electricity prices following the Japanese nuclear leak. While the right panel of Figure 3 shows the estimation of the jump magnitude along with the corresponding 95% SCB, indicating a significant increase in electricity prices at all levels except for high

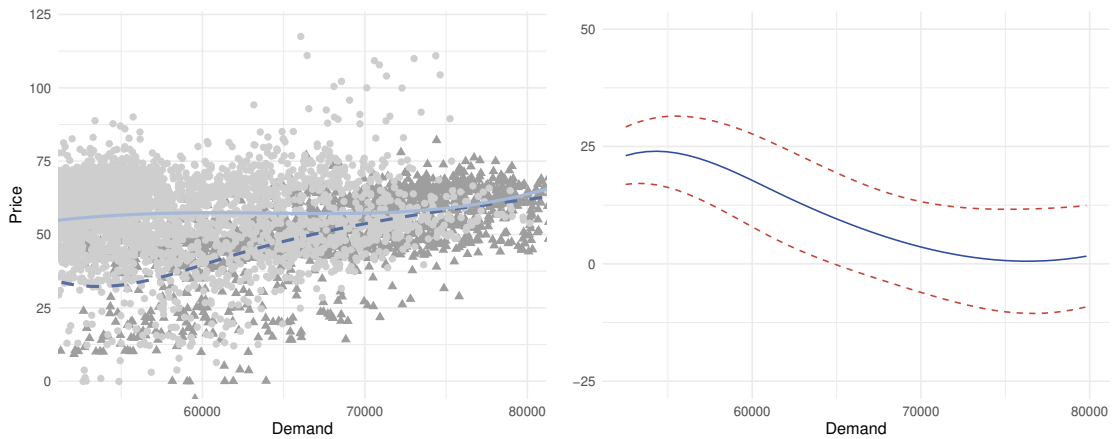


Figure 3: Left panel: The raw data before and after March 15, 2011 (before: triangle markers, after: circle markers), and the corresponding estimation of the mean function (before: dashed line, after: solid line). Right panel: estimation of the jump function with the 95% SCB.

electricity demand.

## 6.2 Temperature data

We illustrate our proposed method on densely observed functional times series by analyzing the temperature data from Sydney in Australia. The dataset we used records the daily maximum and minimum temperatures in Sydney from January 1, 1959, to December 31, 2008, and can be accessed on <http://www.bom.gov.au/climate/data/stations/>. break point detection problem for similar annual temperature curves in Australia has also been investigated in Aue et al. (2018).

After removing the missing data and the data points for February 29th in leap years, we can model the data as a functional time series in (1.1) with  $n = 50$  and  $N_i \leq 365$  for  $i = 1, \dots, n$ . The proposed break point testing procedures both reject the null hypothesis, suggesting that a significant break point in Sydney's temperature climate occurred within the half-century. The location of the year of temperature jump and the estimation of the

jump magnitude are summarized in Table 4 and Figure 4.

	$\mathcal{L}_2$ -test	$\mathcal{L}_\infty$ -test	$\hat{k}_{n,2}$	$\hat{k}_{n,\infty}$
Minimum temperature	< 0.001	< 0.001	1973	1972
Maximum temperature	< 0.001	0.002	1988	1986

Table 4: Summary of results for p-values and location of the break point in Sydney.

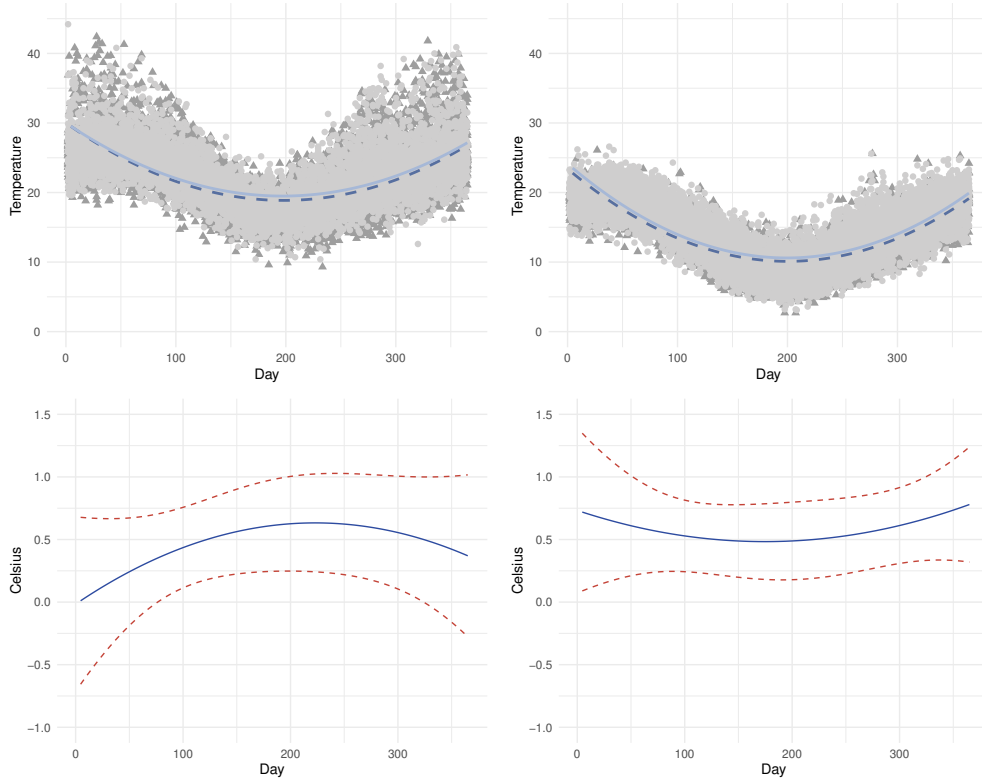


Figure 4: Top-left panel: of the maximum temperature before and after 1988 in Sydney, and the corresponding estimation of the mean function. Top-right panel: the minimum temperature before and after 1973 in Sydney, and the corresponding estimation of the mean function (before: triangle markers, dashed line; after: circle markers, solid line). Bottom panels: estimation of the jump function for the maximum temperature (left) and the minimum temperature (right) with the 95% SCB.

Table 4 and Figure 4 show that the daily minimum temperatures in nearly all seasons

increased by 0.5–1 Celsius around the early 1970s. This could be explained by breaks in the El Niño-Southern Oscillation (ENSO), which is often associated with higher temperatures and typically result in warmer temperatures and reduced rainfall. As Trenberth and Hoar (1996) and Trenberth and Hoar (1997) noted, since the 1970s, breaks in the ENSO pattern began to emerge, with an increase in the frequency of El Niño events and a decrease in La Niña events. Additionally, the results of our method also indicate that the daily maximum temperatures also rose in the late 1980s, with the increase being particularly noticeable in winter, which coincides with the findings in Aue et al. (2018).

## 7 Concluding remark

In this paper, we introduce a unified framework for detecting structural breaks in functional time series from sparse to dense sampling designs. By constructing a smoothed CUMSUM process, we propose test statistics based on the  $\mathcal{L}_2$ - and  $\mathcal{L}_\infty$ -norms and derive their asymptotic properties by modern Gaussian approximation techniques. The corresponding break point estimators are obtained via the argmax functions of the proposed test statistics. Each of these two methods demonstrates either higher power or lower mean absolute error (MAE), respectively, under different types of jump magnitudes. We further develop a simultaneous confidence band for the jump magnitude as a global inference procedure that accommodates arbitrary sampling frequencies. Despite these contributions, several open problems remain. For instance, the inference of the break point itself and the sharp convergence rate for the  $\mathcal{L}_\infty$  break point estimator warrant further investigation. In addition, our methodology can potentially be extended to other settings, such as functional spatial series or locally stationary time series, which provides rich directions for future research.

# Acknowledgements

This research was supported by the National Natural Science Foundation of China awarded 12171269.

# References

- Aue, A., Gabrys, R., Horváth, L., and Kokoszka, P. (2009). Estimation of a change-point in the mean function of functional data. *Journal of Multivariate Analysis*, 100(10):2254–2269.
- Aue, A., Rice, G., and Sönmez, O. (2018). Detecting and dating structural breaks in functional data without dimension reduction. *Journal of the Royal Statistical Society Series B: Statistical Methodology*, 80(3):509–529.
- Baek, C., Kokoszka, P., and Meng, X. (2024). Test of change point versus long-range dependence in functional time series. *Journal of Time Series Analysis*, 45(4):497–512.
- Bai, L., Hu, Q., and Wu, W. (2024+). Inference for structural changes in nonstationary functional time series with partial measurement error. *Manuscript*.
- Bastian, P., Basu, R., and Dette, H. (2023). Multiple change point detection in functional data with applications to biomechanical fatigue data. *arXiv preprint arXiv:2312.11108*.
- Berger, M., Hermann, P., and Holzmann, H. (2023). From dense to sparse design: Optimal rates under the supremum norm for estimating the mean function in functional data analysis. *arXiv preprint arXiv:2306.04550*.
- Berkes, I., Gabrys, R., Horváth, L., and Kokoszka, P. (2009). Detecting changes in the mean

- of functional observations. *Journal of the Royal Statistical Society Series B: Statistical Methodology*, 71(5):927–946.
- Bosq, D. (2000). *Linear processes in function spaces: theory and applications*, volume 149. Springer Science & Business Media.
- Cai, L. and Hu, Q. (2024a). From sparse to dense functional data: Phase transitions from a simultaneous inference perspective. *arXiv preprint arXiv:2401.17646*.
- Cai, L. and Hu, Q. (2024+b). Simultaneous inference for distribution of functional principal scores. *Statist. Sinica*. DOI: 10.5705/ss.202023.0246.
- Cai, T. T. and Yuan, M. (2011). Optimal estimation of the mean function based on discretely sampled functional data: Phase transition. *The Annals of Statistics*, 39(5):2330–2355.
- Cao, G., Yang, L., and Todem, D. (2012). Simultaneous inference for the mean function based on dense functional data. *Journal of nonparametric statistics*, 24(2):359–377.
- Chernozhukov, V., Chetverikov, D., and Kato, K. (2015). Comparison and anti-concentration bounds for maxima of gaussian random vectors. *Probability Theory and Related Fields*, 162:47–70.
- Cui, Y. and Zhou, Z. (2023). Simultaneous inference for time series functional linear regression.
- De Boor, C. (1978). *A practical guide to splines*, volume 27. springer-verlag New York.
- Dette, H. and Wu, W. (2024+). Confidence surfaces for the mean of locally stationary functional time series. *Statistica sinica*. DOI: 10.5705/ss.202023.0150.



- Guo, S., Li, D., Qiao, X., and Wang, Y. (2023). From sparse to dense functional data in high dimensions: Revisiting phase transitions from a non-asymptotic perspective. *arXiv preprint arXiv:2306.00476*.
- Harris, T., Li, B., and Tucker, J. D. (2022). Scalable multiple changepoint detection for functional data sequences. *Environmetrics*, 33(2):e2710.
- Hörmann, S. and Kokoszka, P. (2010). Weakly dependent functional data. *The Annals of Statistics*, 38(3):1845–1884.
- Horváth, L. and Kokoszka, P. (2012). *Inference for functional data with applications*, volume 200. Springer Science & Business Media.
- Horváth, L., Kokoszka, P., and Reeder, R. (2013). Estimation of the mean of functional time series and a two-sample problem. *Journal of the Royal Statistical Society Series B: Statistical Methodology*, 75(1):103–122.
- Hsing, T. and Eubank, R. (2015). *Theoretical foundations of functional data analysis, with an introduction to linear operators*, volume 997. John Wiley & Sons.
- Hu, Q. (2024). Change point analysis of functional variance function with stationary error. *Journal of Multivariate Analysis*, 202:105311.
- Hu, Q. and Li, J. (2024). Statistical inference for mean function of longitudinal imaging data over complicated domains. *Statistica Sinica*, 34:955–982.
- Jiao, S., Chan, N. H., and Yau, C.-Y. (2023). Enhanced change-point detection in functional means. *Statistica Sinica*. DOI: 10.5705/ss.202022.0312.
- Kneip, A. and Liebl, D. (2020). On the optimal reconstruction of partially observed functional data. *The Annals of Statistics*, 48(3):1692–1717.

- Li, D., Li, R., and Shang, H. L. (2023). Detection and estimation of structural breaks in high-dimensional functional time series. *arXiv preprint arXiv:2304.07003*.
- Li, J., Chen, L., Wang, W., and Wu, W. B. (2024).  $\ell_2$  inference for change points in high-dimensional time series via a two-way mosum. *The Annals of Statistics*, 52(2):602–627.
- Li, Y. and Hsing, T. (2010). Uniform convergence rates for nonparametric regression and principal component analysis in functional/longitudinal data. *The Annals of Statistics*, 38(6):3321–3351.
- Liebl, D. (2013). Modeling and forecasting electricity spot prices: A functional data perspective. *The Annals of Applied Statistics*, 7(3):1562–1592.
- Liebl, D. (2019). Nonparametric testing for differences in electricity prices: The case of the Fukushima nuclear accident. *The Annals of Applied Statistics*, 13(2):1128–1146.
- Madrid Padilla, C. M., Wang, D., Zhao, Z., and Yu, Y. (2022). Change-point detection for sparse and dense functional data in general dimensions. *Advances in Neural Information Processing Systems*, 35:37121–37133.
- Mies, F. and Steland, A. (2023). Sequential gaussian approximation for nonstationary time series in high dimensions. *Bernoulli*, 29(4):3114–3140.
- Rice, G. and Zhang, C. (2022). Consistency of binary segmentation for multiple change-point estimation with functional data. *Statistics & Probability Letters*, 180:109228.
- Schumaker, L. (2007). *Spline functions: basic theory*. Cambridge university press.
- Sharghi Ghale-Joogh, H. and Hosseini-Nasab, S. M. E. (2021). On mean derivative estimation of longitudinal and functional data: from sparse to dense. *Statistical Papers*, 62(4):2047–2066.

- Trenberth, K. E. and Hoar, T. J. (1996). The 1990-1995 el niño-southern oscillation event: Longest on record. *Geophysical research letters*, 23(1):57–60.
- Trenberth, K. E. and Hoar, T. J. (1997). El niño and climate change. *Geophysical Research Letters*, 24(23):3057–3060.
- Wang, M., Harris, T., and Li, B. (2023). Asynchronous changepoint estimation for spatially correlated functional time series. *Journal of Agricultural, Biological and Environmental Statistics*, 28(1):157–176.
- Xue, G., Xu, H., and Yu, Y. (2024). Change point localisation and inference in fragmented functional data. *arXiv preprint arXiv:2405.05730*.
- Zhang, H. and Li, Y. (2022). Unified principal component analysis for sparse and dense functional data under spatial dependency. *Journal of Business & Economic Statistics*, 40(4):1523–1537.
- Zhang, X. and Wang, J.-l. (2016). From sparse to dense functional data and beyond. *The Annals of Statistics*, 44:2281–2321.
- Zhou, Z. and Dette, H. (2023). Statistical inference for high-dimensional panel functional time series. *Journal of the Royal Statistical Society Series B: Statistical Methodology*, 85(2):523–549.